Winter 12-14-2018

Combination Therapy: PARP Inhibitor Synergizes the Therapeutic Efficacy of Doxorubicin in the treatment of Prostate Cancer

Momin Ansare
Pittsburg State University, mansare@gus.pittstate.edu

COMBINATION THERAPY: PARP INHIBITOR SYNERGIZES THE THERAPEUTIC EFFICACY OF DOXORUBICIN IN THE TREATMENT OF PROSTATE CANCER

A thesis submitted to the Graduate School
in Partial Fulfillment of the Requirements
for the Degree of
Master of Science in Chemistry

Momin Ansare

Pittsburg State University

Pittsburg, Kansas

November 2018

COMBINATION THERAPY: PARP INHIBITOR SYNERGIZES THE THERAPEUTIC EFFICACY OF DOXORUBICIN IN THE TREATMENT OF PROSTATE CANCER

Momin Ansare

APPROVED:

Thesis Advisor: _____
Dr. Santimukul Santra, Department of Chemistry

Committee Member: _____
Dr. Tuhina Banerjee, Department of Chemistry

Committee Member: _____
Dr. Irene Zegar, Department of Chemistry

Committee Member: _____
Dr. Phillip Harries, Department of Biology

ACKNOWLEDGMENTS

I would first like to thank Dr. Santimukul Santra for his support, guidance and teaching through the course of my master's degree and research project. He selected and designed a project that was suitable for my interest and beneficial for my progression as a scientist in the future. I would also like to thank Dr. Tuhina Banerjee for a great amount of assistance in explaining many complex concepts pertaining to this project to me, and also for being a very helpful and informative instructor for my biochemistry course. I would also like to thank Dr. Irene Zegar, Dr. William Shirley, Dr. Charles Neef, Dr. James Mcafee, Dr. Kristopher Mijares ,Dr. Dilip Paul, Dr. Khamis Siam for support throughout my master's degree as instructors and while working with them as a teaching assistant.

I would also like to thank my peers, Tanuja Tummala, Saloni Darji, Sneha Ramanujam, and Zach Shaw for collaboration and support. I would also like to thank my family, especially my mother Iffat Ansare and my sister, Momina Sims.

COMBINATION THERAPY: PARP INHIBITOR SYNERGIZES THE THERAPEUTIC EFFICACY OF DOXORUBICIN IN THE TREATMENT OF PROSTATE CANCER

An Abstract of the Thesis by
Momin Ansare

The cancer that men are most susceptible to in the United States is prostate cancer. Common treatment options for prostate cancer include surgery, hormone therapy, chemotherapy, and radiation therapy. Recently however, the nanoparticles have shown promising applications in overcoming the drawbacks of the currently available treatment options. We tried to enhance the capability of the nanoparticle formulation by loading them with a novel drug combination for the treatment of prostate cancer. Herein, we synthesized folate conjugated iron oxide nanoparticles encapsulated with doxorubicin and olaparib for imaging and targeted treatment of prostate cancer. Both drugs are approved by the FDA for clinical cancer treatment. IONPs coated with polyacrylic acid were synthesized with water-based precipitation method, followed by functionalization with folate using “click” chemistry. Briefly, the IONPs were first propargylated using EDC/NHS carbodiimide chemistry followed by CuI catalyzed “click” chemistry using azide-functionalized folic acid. Next, doxorubicin and olaparib were co-encapsulated in the IONPs using the solvent diffusion method. The resulting therapeutic nanomedicines were characterized by measuring size, zeta potential, and UV/fluorescence emission and absorbance. The two drugs were used together to explore if the synergistic effect they normally have was still in effect while they were encapsulated in nanoparticles. Cytotoxicity was explored through MTT assay, and cell uptake studies. The nature of the cell death was observed through apoptosis, ROS, and comet assay studies. Finally, the antimetastatic potential of the therapeutic nanoparticles was studied via migration assay and reported.

Table of Contents

LIST OF FIGURES

FIGURE **PAGE**

Chapter I

1 INTRODUCTION:

1.1 Prostate Cancer: Understanding, and Treatment Options

Prostate cancer is the most common cancer affecting men in the United States. It has many classifications including adenocarcinoma, transitional cell, squamous cell, and small cell prostate cancers.[1-6] Adenocarcinoma prostate cancer can be acinar adenocarcinoma or ductal adenocarcinoma, which is characterized by cribriform, or papillary architecture lined by columnar pseudostratified malignant epithelium.[7] Ductal adenocarcinoma occurs more often with advanced stage cancer. It is sometimes diagnosed via needle biopsy.[8]

Treatments options for prostate cancer include surgery, hormone therapy, chemotherapy, and radiation therapy; the most common option is the radical prostatectomy.[9-17] If the disease persists after radical prostatectomy, chemotherapy is introduced.[15] Drugs that have been used to treat prostate cancer include Docetaxel, cabazitaxel, mitoxantrone, Estramustine, etoposide, and doxorubicin. [18]

Mitoxantrone has typically been used in combination with either prednisone or estramustine.[19] These combinations have had success in reducing the pain a patient feels from castration-resistant(cancer that persists after a prostatectomy) prostate cancer.[19] Docetaxel has also been used to combat castration-resistant prostate cancer in combination with either estramusine or prednisone.[19] Patients with castration-resistant prostate cancer treated with docetaxel cocktails have been shown to have an increased longevity when compared to such patients treated with mitoxantrone cocktails.[19] Cancer cells can become resistant to taxanes if they express P-glycoprotein (P-gp). Cabazitaxel has poor affinity for P-gp compared to docetaxel, hence it has been shown to retain activity in docetaxel-resistant tumors.[20]

1.2 Nanotechnology: Prospects for Improved Treatment

Nanotechnology has promising applications for improving prostate cancer treatment. Nanoparticles can be used to improve the efficacy of chemotherapy, by carrying encapsulated drugs to targeted cells. Many targeting ligands including amino acids, antibodies, and proteins are being used for drug delivery.[21-26] Iron oxide nanoparticles (IONPs) have multimodal functionalities. In addition to being able to carry drugs by functionalizing with targeting ligands, they can also be used as contrast agents in MRI imaging due to their superparamagnetic properties.[6] Gold nanoparticles (AuNPs) also have potential to deliver drugs in cancer treatment. Like IONPs, polymer coated-AuNPs can also carry small molecular weight drugs, and these polymer coatings can be functionalized with targeting ligands to selectively accumulate chemotherapy drugs at the tumor site, thus reducing side effects on healthy cells.[22] Polymeric nanoparticles are also being used for drug delivery in a similar fashion to IONPs and AuNPs.[21,22] Nanoparticles with high-atomic-number element can be used as radiosensitizer due to their stronger photoelectric effects on soft tissues under gamma irradiation. This is proposed to increase the efficiency of radiotherapy.[28]

1.2.1 Polymeric Nanoparticles Used for Drug Delivery

Poly (lactic-co-glycolic acid)- curcumin(CUR) nanoparticles (PLGA-CUR NPs) (**Figure 1**) have been shown to inhibit proliferation and colony formation of prostate cancer.[29] These effects have been shown to be greater in PLGA-CUR NPs than in free curcumin. Prostate cancer cells treated with these NPs showed evidence of PARP cleavage as well as inhibition of anti-apoptotic proteins as Bcl-X_L and Mcl-1.[1]

The internalization of the PLGA-CUR NPs in DU154 prostate cancer was shown in a time dependent fashion. Within one hour, PLGA-CUR NPs were substantially engulfed within the cells. By the next three hours, they were fully internalized. At the eighteenth-hour, PLGA-CUR NPs were located near the cell nuclei. As shown in **Figure 1C** the extent of endocytosis is shown to be dependent on the prostate cancer cell lines. PLGA-CUR NPs were shown to internalize more effectively in DU-145 cells than in PC-3 and C4-2. As seen in **Figure 1D** fluorescence intensity of cells treated with PLGA-CUR NPs had a higher fluorescence intensity compared with

cells treated with free curcumin. **Figure 1E** shows TEM images wherein extensive production of vacuoles was observed.

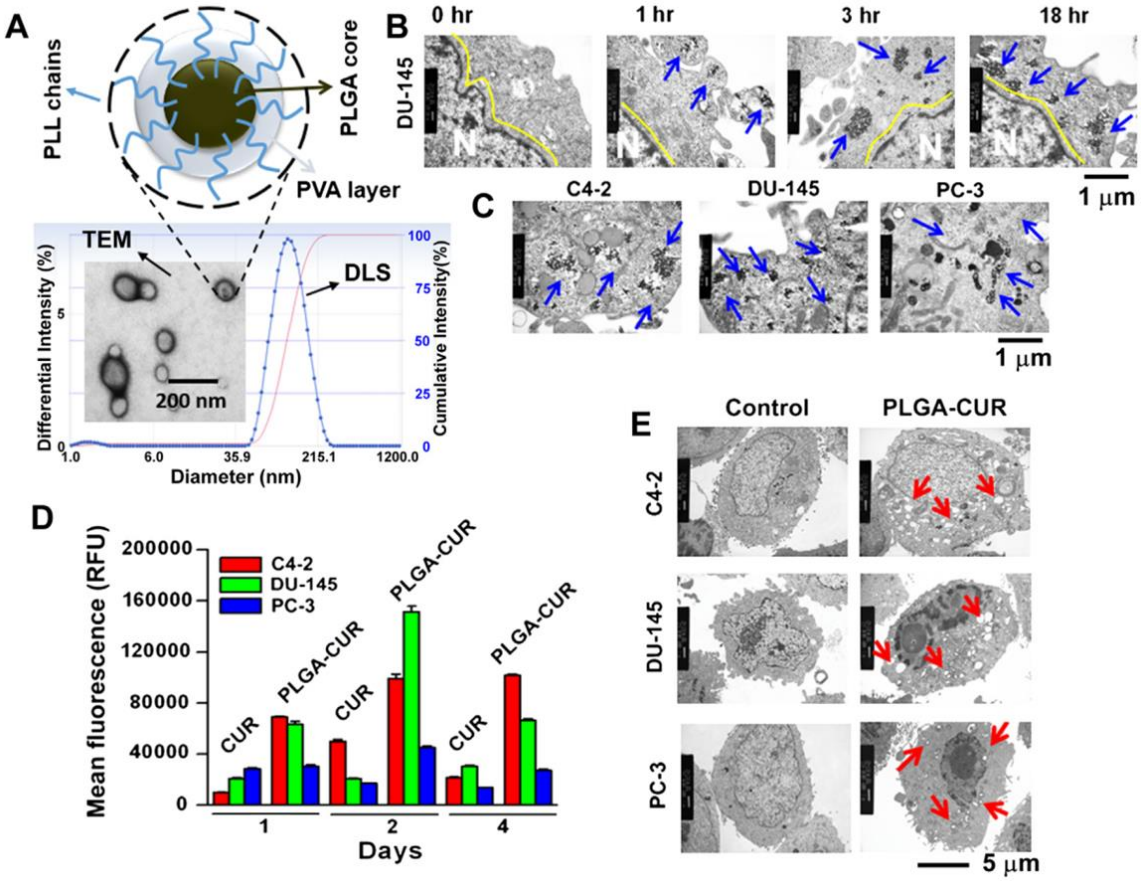

Figure 1: (A) Hypothetical structure of PLGA-CUR NPs and the particle size, (B) time dependent internalization of PLGA-CUR NPs, (C) PLGA-CUR NPs accumulation in different types of prostate cancer cells, (D) PLGA-CUR NPs cellular uptake compared to that of curcumin, (E) alteration of cellular structures due to treatment with PLGA-CUR NPs.

Conjugating PLGA-CUR NPs with monoclonal antibodies increases the cell internalization, indicating better efficacy and targeting. This is shown in **Figure 2A** by comparing mean fluorescence from PC-3 and C4-2 cells treated with PLGA-CUR NPs and PSMA-PLGA MAb -CUR NPs. **Figure 2B** shows PSMA-PLGA MAb -CUR NPs internalization in the PSMA+ C4-2 cells more than in PSMA- PC-3 cells using fluorescent microscopy. **Figure 2C** shows in both PC-3 and C4-2 cells, PSMA-PLGA MAb -CUR NPs decrease the cells viability more than PSMA-PLGA -CUR NPs.

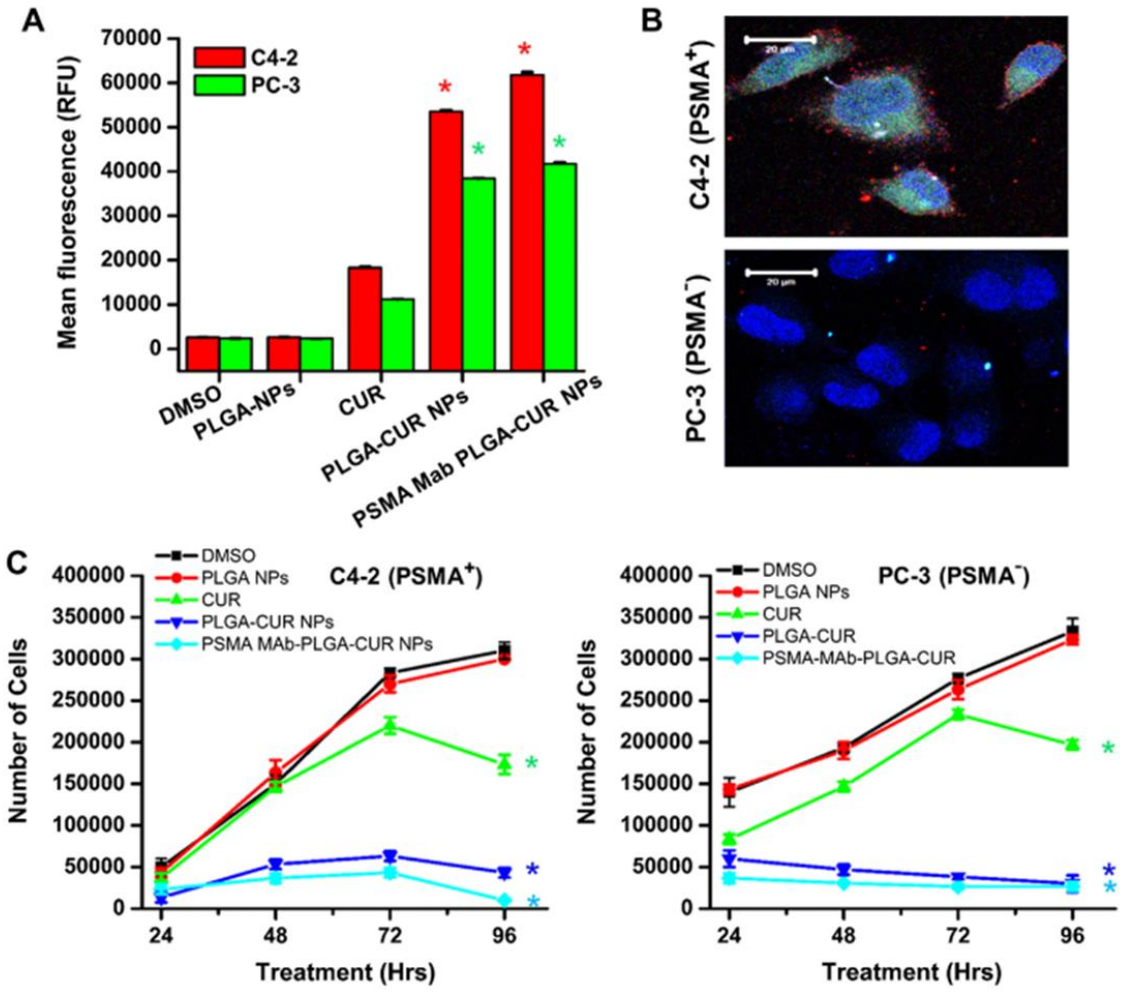

Figure 2: (A) internalization of PSMA-MAb PLGA-CUR NPs in C4-2 and PC-3 cancer cells, (B) cell internalization via fluorescent microscopy, (C) cell viability of cells treated with PSMA-MAb PLGA-CUR NPs.

Similar study on cell viability was performed where synergistic effect of docetaxel and curcumin encapsulated nanoparticles were shown in **Figure 3**.[30]

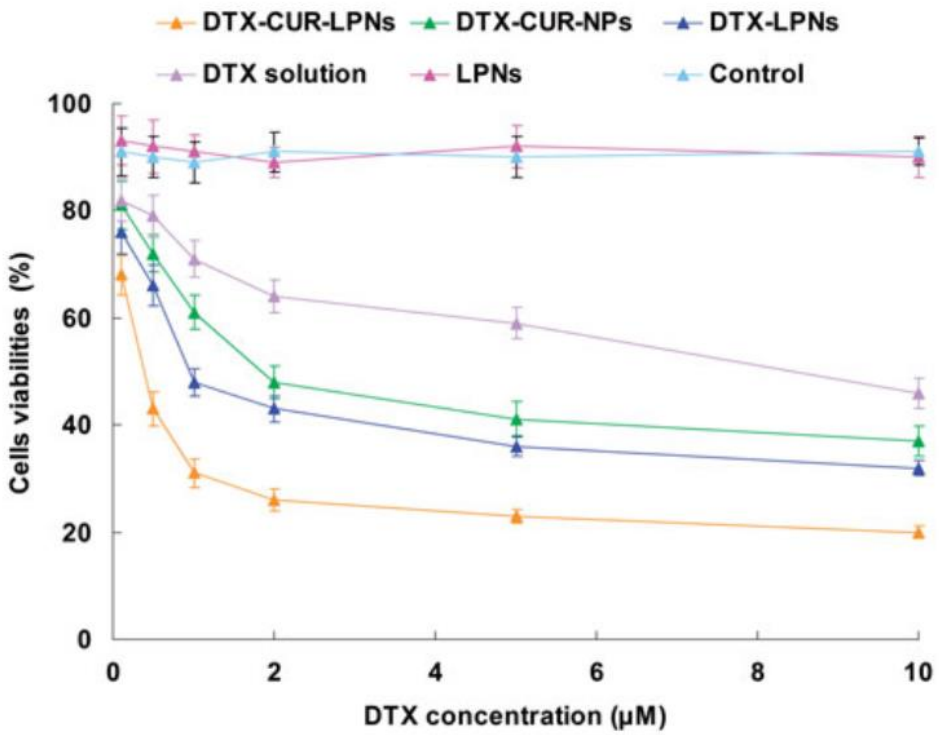

Figure 3: Cell viability assay in vitro cytotoxicity experiments of LPNs, NPs, and free drugs.

1.2.2 Gold Nanoparticles Used for Drug Delivery

Application of gold nanoparticles to prostate cancer treatment are also reported in literature. Gold nanoparticles conjugated with epigallocatechin gallate (EGCG), Gelatin, and doxorubicin to produce epigallocatechin gallate gelatin-doxorubicin conjugate (GLT-DOX)-coated gold nanoparticles (DOX-GLT/EGCG AuNPs).[31] The scheme of the synthesis of the nanoparticles is given in **Figure 4** along with the optical properties. EGCG AuNPs were prepared by reduction of tetrachloroaurate (III) ions in EGCG aqueous solution. GLT-DOX conjugate was synthesized by combining GLT and citraconic anhydride, followed by an EDC-NHS addition before finally being bonded to doxorubicin. DOX-GLT/EGCG AuNPs significantly inhibit the proliferation of PC-3 cancer cell. The release of doxorubicin could be tracked by monitoring the recovery of its fluorescence signal between the emission range of 560-580nm. The efficacy of DOX-GLT/EGCG AuNPs for treating prostate cancer is shown in **Figure 5** via the concentration

dependent cell viability diagram for PC-3 cells treated with free DOX, GLT-DOX/AuNPs and GLT-DOX/EGCG-AuNPs at different DOX equivalents.

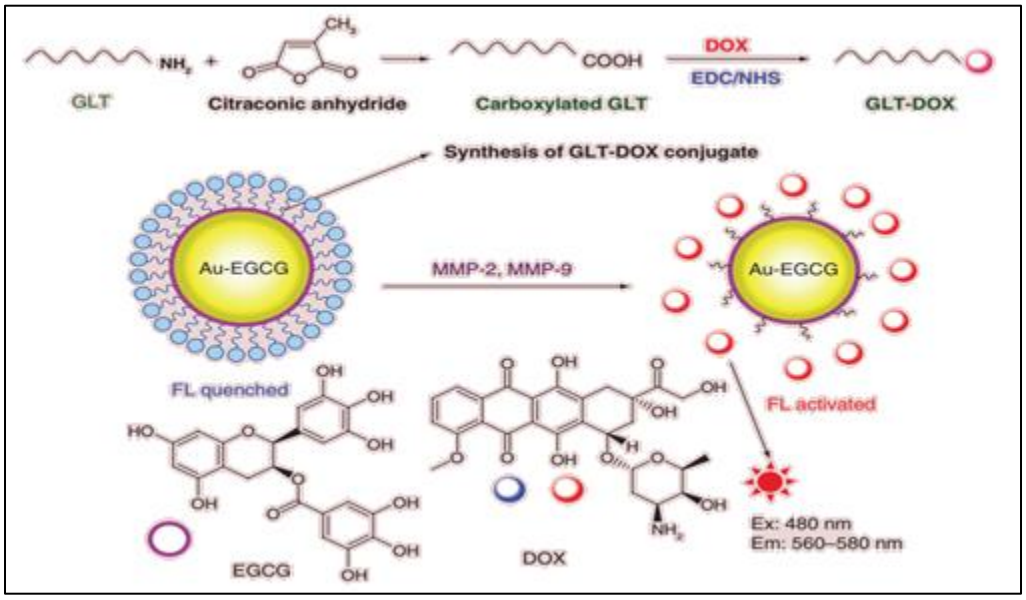

Figure 4 Scheme of the synthesis and optical properties of layer-by-layer assembled GLT-DOX/EGCG-AuNPs.

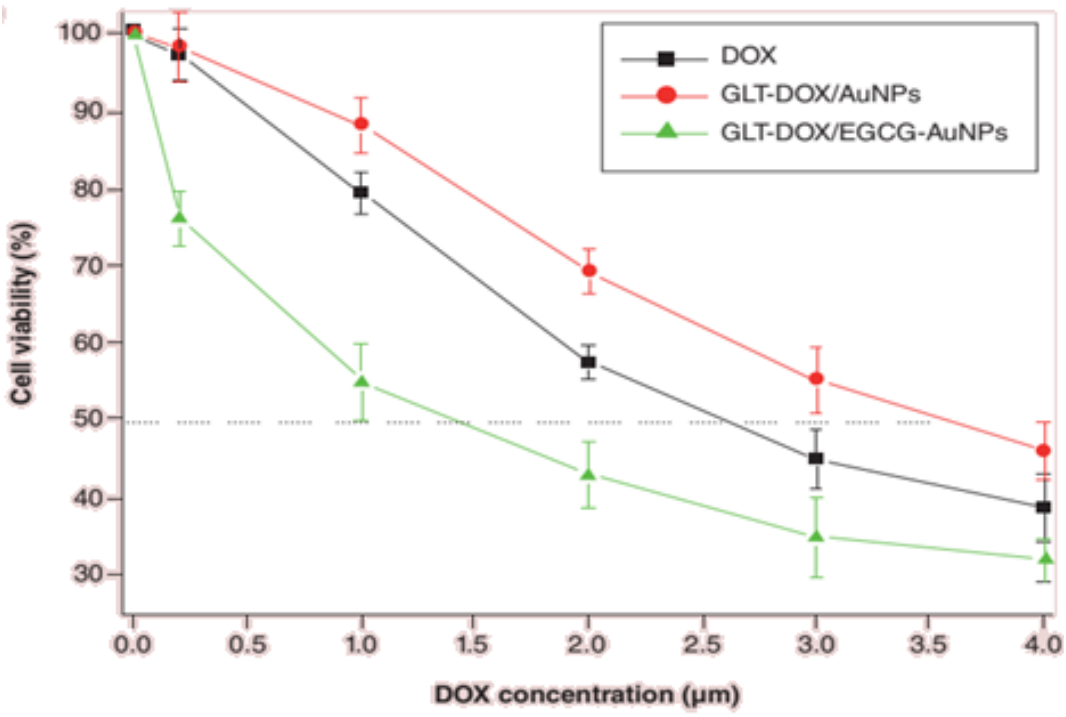

Figure 5: Shows cell viability of PC-3 cells treated with free DOX, GLT-DOX/AuNPs and GLT-DOX/EGCG-AuNPs using different concentrations of DOX.

1.2.3 Multimodal Iron Oxide Nanoparticles for the Drug Delivery and Tumor Imaging

Applications of super paramagnetic iron oxide nanoparticles to treat cancer are also a high-interest topic with many research projects underway; they have been shown to be useful for both drug delivery and diagnostic imaging.[32, 33] Iron oxide magnetic nanoparticles (MNPs) were conjugated with J591, an antibody to an extracellular epitope of PSMA, to enhance the targeted delivery of drugs and MRI imaging of prostate cancer. Orthotopic tumor-bearing NOD.SCID mice were injected intravenously with J591-MNPs, or non-targeting MNPs and MRI studies were performed on these mice at 2 hours and 24 hours after injection. The prostate cancer cell viability was shown not to be affected by the J951-MNPs, nor was the antibody specificity compromised. However, cellular iron uptake was shown to be enhanced as a result. **Figure 6** shows MRI images of non-tumor-bearing mice. The prostate is shown to darken over time indicating accumulation of MNPs.

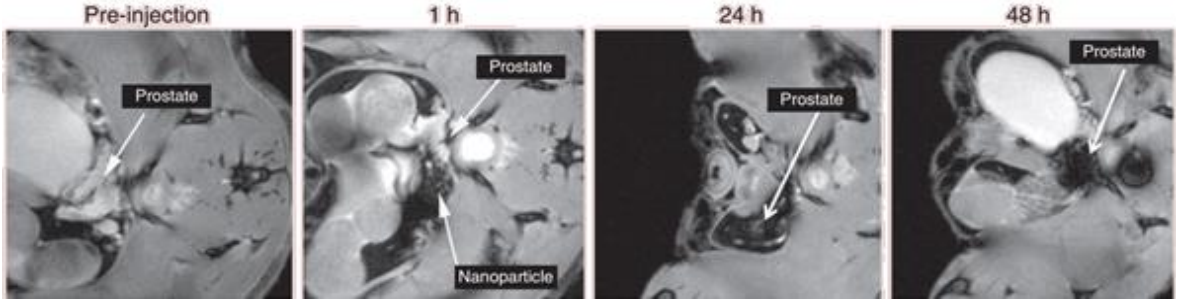

Figure 6: Shows MRI images of non-tumor bearing mice following direct injection of magnetic nanoparticles into prostate.

Prostate specific membrane antigen (PSMA) targeted superparamagnetic iron oxide nanoparticle (SPION) loaded with Docetaxel (J591-SPION-Dtxl) demonstrated to be an effective MRI contrast agent in prostate cancer imaging.[33] Docetaxel was chosen because it is the most commonly used chemotherapy drug for treating prostate cancer. Upon treating cells with SPIONs(J591-SPION-Dtxl), apoptosis associated protein expression was observed. Down-regulation of anti-apoptotic proteins inhibits chemo-resistance associated proteins. **Figure 7A** and **7B** shows the scheme of the synthesis for SPIONs(J591-SPION-Dtxl) and TEM images of the particles respectively. The size and zeta potential were measured by DLS as shown in **Figure 7C**

and **Figure7D**. An FTIR spectrum is shown in **Figure 7E** which helps to confirm the nanoparticles were properly synthesized. Thermogravimetric analysis in **Figure 7F** confirms the loading of Dtxl

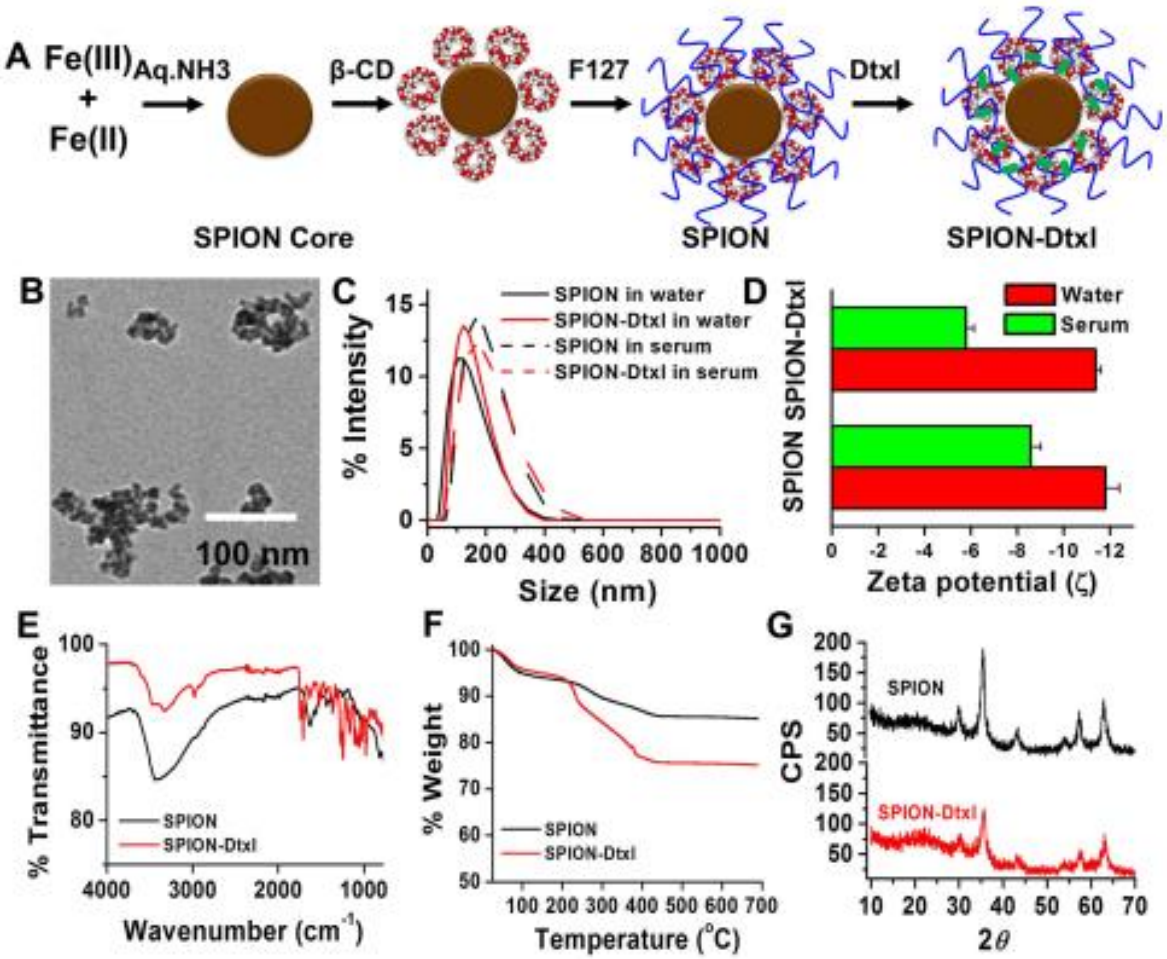

in the SPOIN, which had greater weight loss than SPION. X-ray diffraction patterns of SPION and SPION-Dtxl are shown in **Figure 7G**. **Figure 8** shows the noticeably less concentration dependent proliferation of C4-2 cells and PC-3 cells treated with SPION-Dtxl as compared with free Dtxl.

Figure 7: (A) Schematic of hypothetical structure and synthesis of SPION-Dtxl, (B) Transmission electron microscopic image of SPION-Dtxl , (C) Particle size potential of SPION and SPION-Dtxl in water and serum,(D) Particle zeta potential of SPION and SPION-Dtxl in water and serum, (E) FT-IR spectra of SPION and SPION-Dtxl, (F) Thermogravimetric analysis of SPION and SPION-Dtxl, and (G) X-ray diffraction patterns of SPION and SPION-Dtxl. The success of specific targeting of

SPION-Dtxlto PSMA+PC cells and tumor tissues shows promise for future development of SPION-Dtxl as a targeted therapy for prostate cancer.[33]

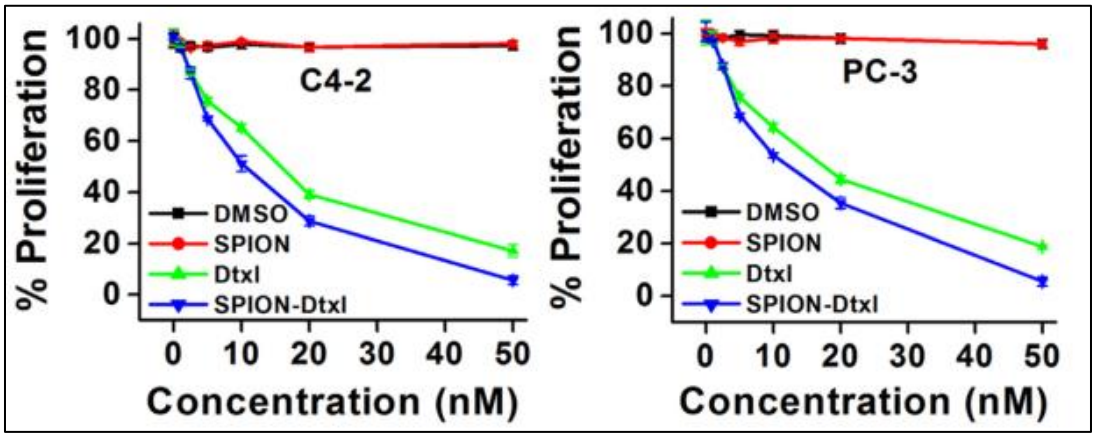

Figure 8: The concentration dependent proliferation of C4-2 cells and PC-3 cells treated with SPION-Dtxl as compared with free Dtxl.

In this study, we synthesized a novel nanoformulation that retains higher efficiency in killing the metastatic prostate cancer cells. First, we conjugated superparamagnetic iron oxide nanoparticles (IONP-Fol) with folate to achieve targetability of the prostate cancer cells that overexpress folate receptors. Then, we encapsulated the nanoparticle with drug cocktail containing olaparib and doxorubicin which were found to be the most effective chemotherapeutic agents against LNCaP. The combination of these drugs could possess a good synergetic effect because of their complementary mechanisms of action. The cytotoxicity of doxorubicin is primarily due to DNA damage, and olaparib, being a PARP inhibitor, prevents repair of DNA damage. Thus the DNA damage due to doxorubicin will not be resisted by PARP. It is also proposed that encapsulating these two drugs into nanoparticles will improve the delivery and therapeutic efficacy of the drugs significantly.

Chapter II

Combination Therapy: PARP Inhibitor Synergizes the Therapeutic Efficacy of Doxorubicin in the Treatment of Prostate Cancer

2.1 Introduction:

2.1.1 Introduction to PARP inhibitors

PARP inhibitors have been of interest in potential treatment for various types of cancers, both as monotherapy or in combination with other chemotherapy drugs.[34,43] Poly (ADP-ribose) polymerase proteins are essential players in DNA repair. [34,43] They bind to DNA once a single strand break is detected, and then produce polymeric adenosine diphosphate ribose by undergoing a conformational change. This in-turn activates other DNA repair enzymes including DNA ligase III and DNA polymerase beta. [34,43]

2.1.2 Olaparib and Doxorubicin

Olaparib (structure shown in **Figure 1**[34]) is one of the PARP inhibitors which acts by blocking the enzymatic function of PARP. It stalls and collapses DNA replication forks, thus inducing double strand breaks. It is particularly useful for programmed cell death of cells lacking homologous DNA repair. Cells with BRCA1 and BRCA2 mutations are thought to be poor in such repairs, and some prostate cancers have been found to have such mutations. The effectiveness of olaparib as an anticancer drug is primarily dependent on the amount that reaches the intercellular compartment. It is proposed that encapsulating olaparib into targeted nanoparticles would highly increase the efficacy of the drug.[34]

Doxorubicin (structure shown in **Figure 1**[37]) has various cytotoxic effects including topoisomerase II inhibition which induces supercoiling of DNA, free radical generation, DNA unwinding/separation, inhibition of macromolecule production, and increase in alkylation.[35]

Although these cytotoxic effects are quite useful for fighting cancer, they also have many negative effects on the healthy parts of the body. These negative side effects include phlebosclerosis, production of necrotic tissue, damage to the immune system, cellulitis, and damage to the heart, brain, liver and kidney. It has been found to cause cardiomyopathy even 17 years after treatment. Using nanoparticles to target cancer cells specifically with doxorubicin as the cargo is proposed to reduce the extent of the side effects significantly.[36]

2.1.3 Synergistic Effect of Treatment with Doxorubicin in Combination with Olaparib

Since Doxorubicin is effective at inducing DNA damage and olaparib is effective at inhibiting DNA repair, it is proposed that treatment with a combination of the two drugs will have a much higher rate of cytotoxicity, thus displaying a synergistic relation between the two drugs in relation to cancer treatment.

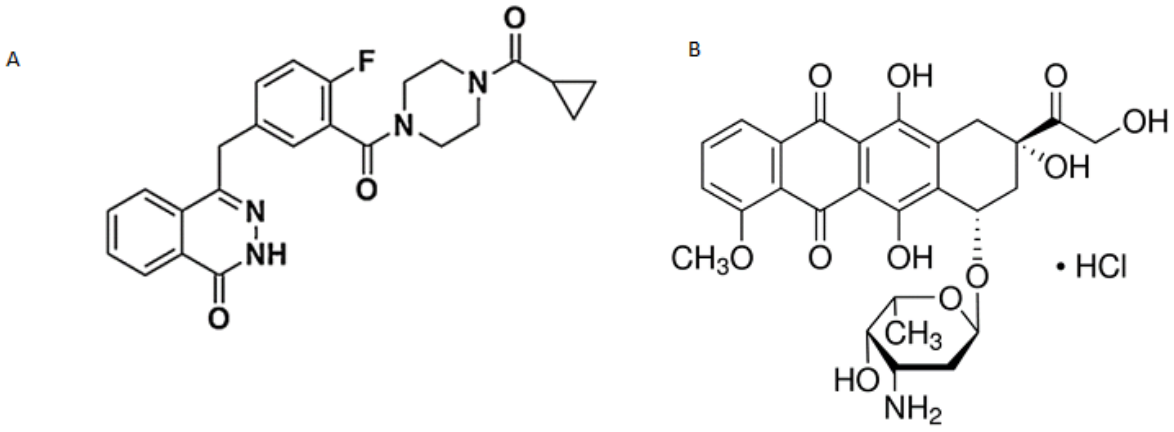

Figure 1: Shows chemical structures of olaparib (A) and doxorubicin (B).

LNCaP is a cell line of prostate cancer that has been found to have an overexpressed folate receptor. Folate ligands on nanoparticles are found to be effective in targeting LNCaP cells specifically with both chemotherapy drugs. This has been shown by observing the internalization of the nanoparticles as well as their viability over time after treatment. Iron oxide nanoparticles coated with poly acrylic acid have been shown in many studies to be both effective in targeted drug delivery as well as bio-compatible.

In this work, poly acrylic acid-coated iron oxide nanoparticles were synthesized using water-based precipitation method as well as functionalized with folate using EDC/NHS and click

chemistry for targeting. The folate conjugated iron oxide nanoparticles (IONP-Fol) were then used to encapsulate both doxorubicin and olaparib. A scheme for the hypothetical structure, synthesis and design of the nanoparticles is given in **Figure 2**. The photoactive properties of doxorubicin made it possible to confirm it's encapsulation by UV/fluorescence studies. Dynamic light scattering (DLS) studies were also conducted to test the appropriate size for encapsulation, and entry/exit in and out of the cell. The zeta potential of the nanoparticles was also observed by DLS to confirm functionalization with folate. The size was also observed over the course of 60 days to confirm that the nanoparticles would be stable during the course of a typical chemotherapy cycle.

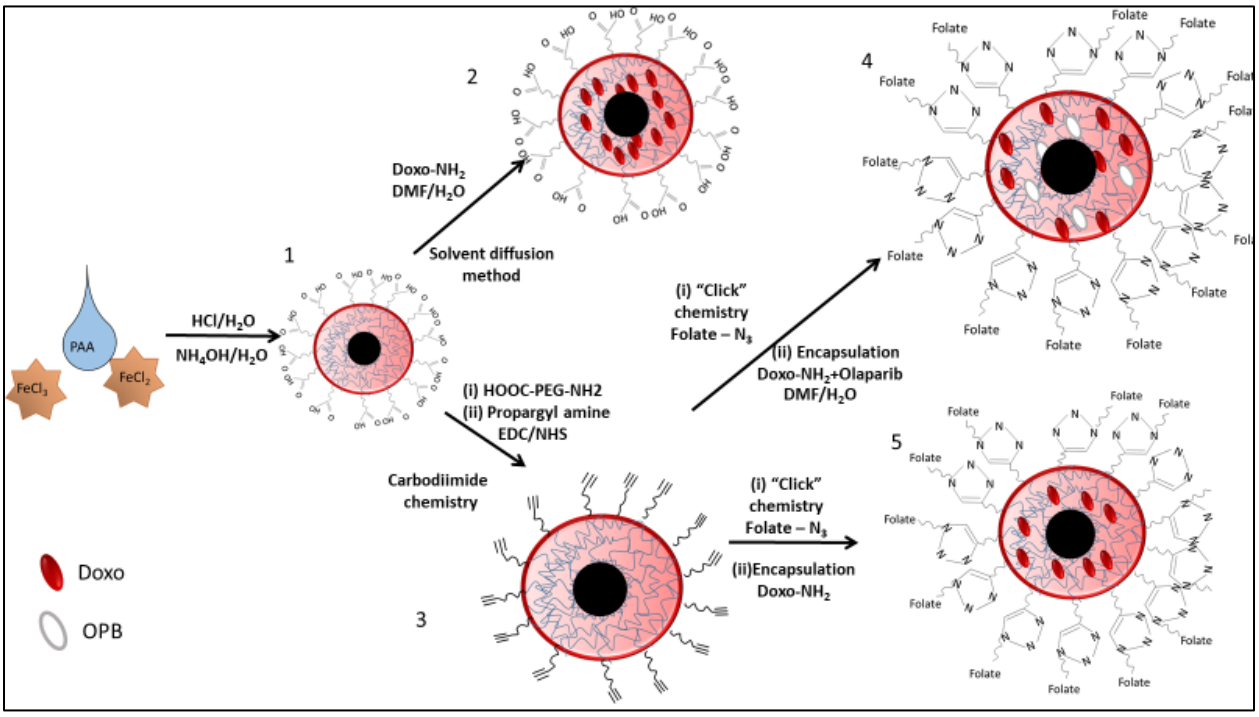

Figure 2: Shows a scheme for the hypothetical structure, synthesis and design of the nanoparticles.

The photoactive properties of doxorubicin were utilized to observe the internalization of the nanoparticles in LNCAP cells via fluorescent microscopy as shown in **Figure 9**. Alongside the confirmation of internalization, the viability of the cells over time was observed via MTT assay. Since oxidative stress has been found to be the result of treatment of doxorubicin in other studies, the level of the reactive oxidative species in the cell culture was also observed over

time. Studies to detect whether the mode of programmed cell death was apoptosis or necrosis were also conducted. Since the primary mechanism of action for both drugs in the cocktail involve DNA damage, the extent of DNA damage caused by the functionalized therapeutic nanoparticles was observed via comet assay. Finally, due to the highly metastatic nature of prostate cancer, particularly when it is castration-resistant, the antimetastatic potential of the drug carrying IONP-Fol particles was tested via migration assay.

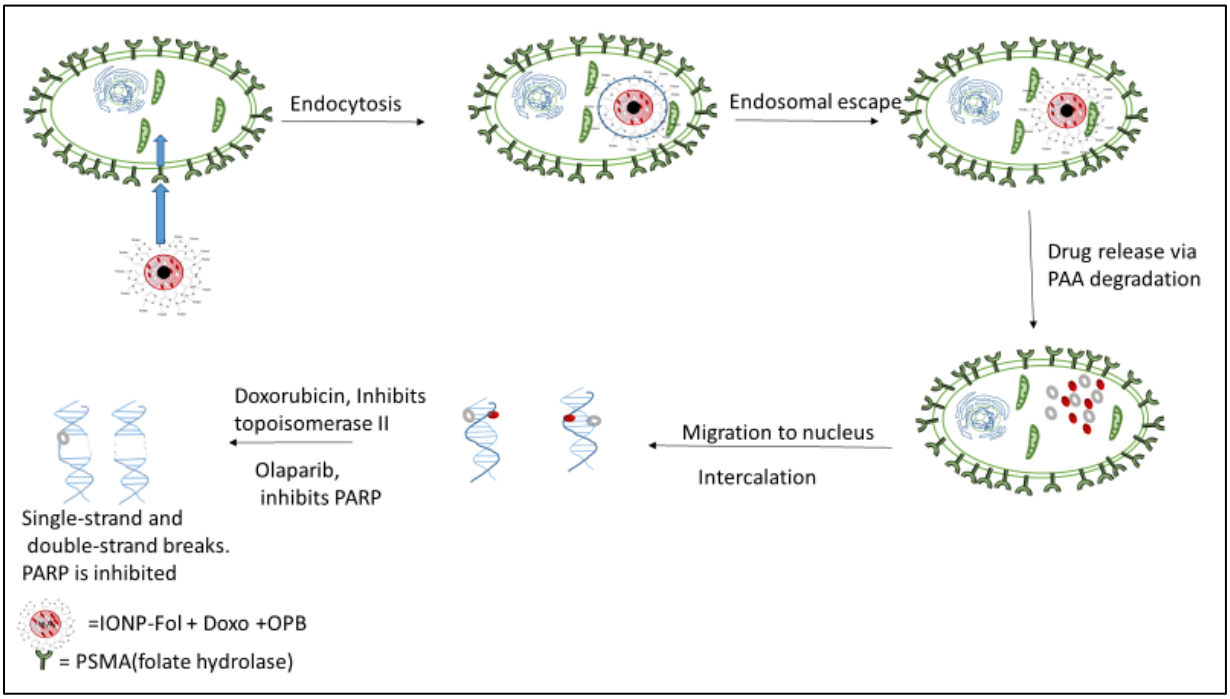

Figure 3: Mechanism of action: A scheme of the cellular internalization of the nanoparticles, and therapeutic actions of the released drugs.

2.2 Results and discussion:

2.2.1 Synthesis and Characterization of IONP:

The polyacrylic acid (PAA) coated super paramagnetic iron oxide nanoparticles (IONP) were synthesized and purified similarly to what is described in previously reported methods.[42] The size of the PAA-coated IONPs was measured using dynamic light scattering and determined to be 46.99 ± 2nm (**Figure 4A**). The zeta potential which was found to be -19.9mV confirms the PAA coating on the surface of nanoparticle (**Figure 4B**).

PAA coated IONPs were functionalized with folate via EDC/NHS and click chemistry as per **Figure 1.** The size of the folate functionalized IONPs was found to be 49.25 ± 2nm via dynamic light scattering **(Figure 4C)**. The zeta potential was found to be -21.0 mV **(Figure 4D)**, and as expected negativity decreased after the folate conjugation. The presence of folate was confirmed via UV absorbance and emission at approximately 350nm(**Figure 5A**) and 340nm(**Figure 5B**) respectively using UV spectroscopy.

Doxorubicin and Olaparib were encapsulated into the nanoparticles using the solvent diffusion method. The folate-functionalized IONP encapsulated with doxorubicin and olaparib (fol-IONP-DOXO-OLA) thus synthesized was purified using dialysis technique. The size was found to be 51.86 ± 2nm**(Figure 4E)** whereas the zeta potential was found to be -24mV **(Figure 4F)**. The encapsulation of the doxorubicin was confirmed by its ultra violet (UV) absorbance of 480nm **(Figure 5C)** and fluorescence emission wavelength of 590nm **(Figure 5D)**.

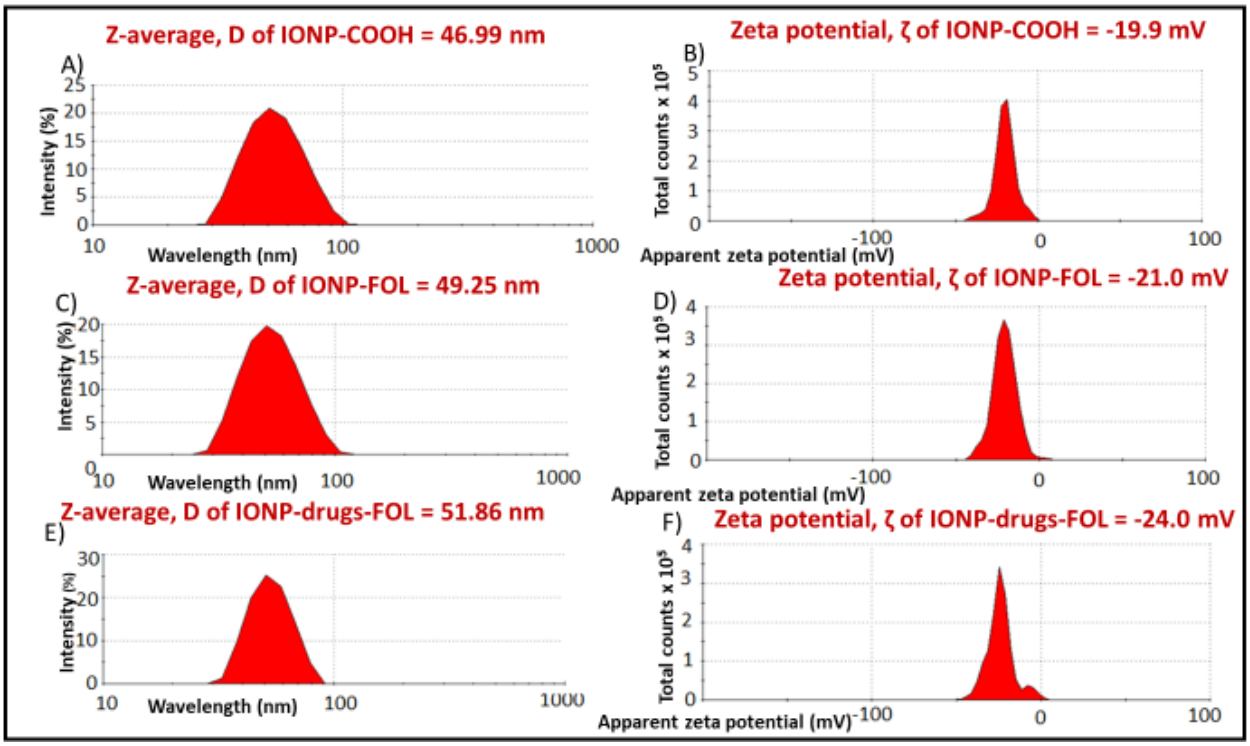

Figure 4: Size (A, C, E) and Zeta potential (B, D, F) data for IONP-COOH, IONP-FOL, and IONP - FOL encapsulating drug cocktail collected using dynamic light scattering.

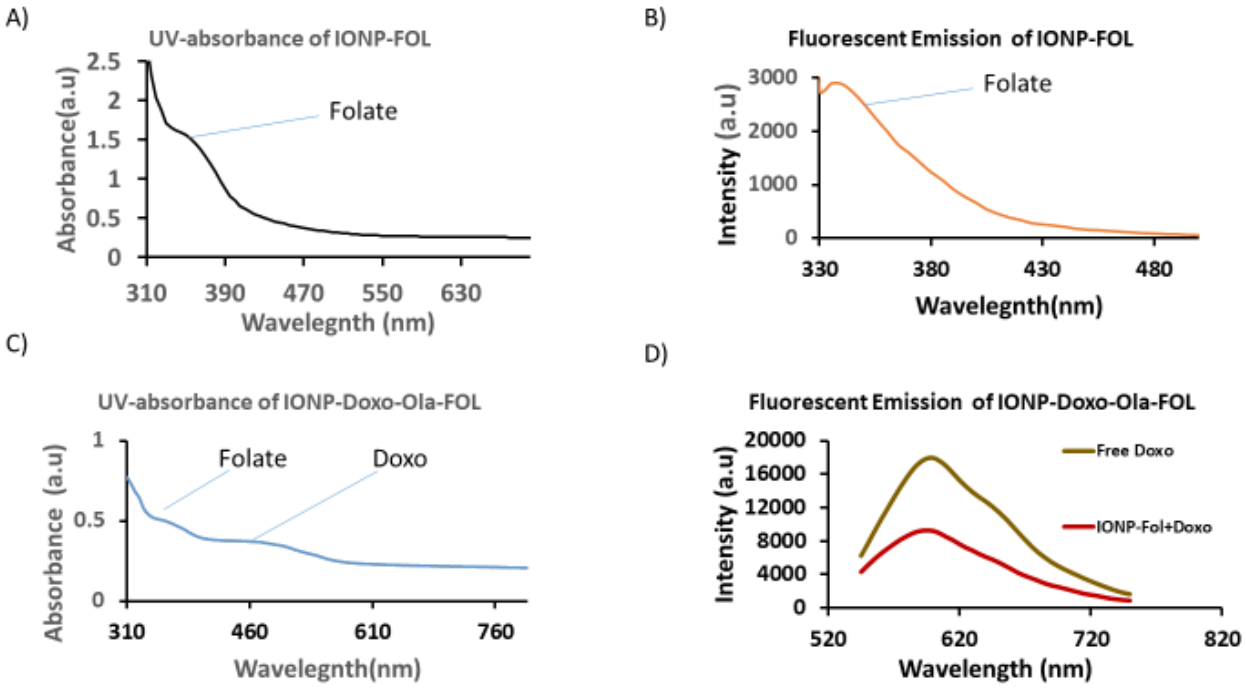

Figure 5: UV-Visible absorption and fluorescence emission characterization. A) UV-visible absorption spectra for IONP-FOL. B) Fluorescence emission spectra for IONP-FOL. C) UV-visible absorption for IONP-DOXO-OLA-FOL. D) Fluorescence emission spectra for IONP-DOXO-OLA-FOL.

2.2.2 Stability Studies:

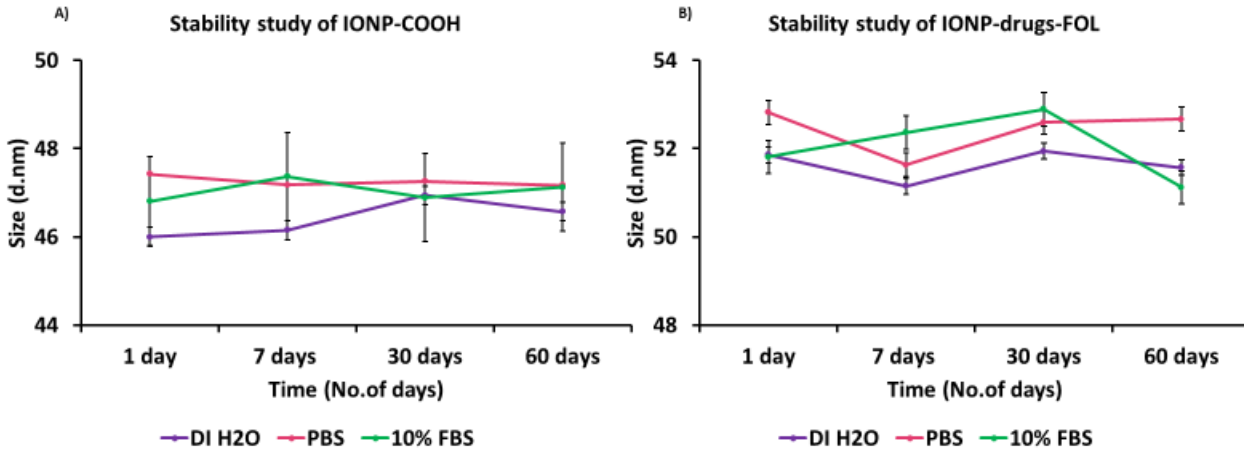

Figure 6: Size stability studies for (A) IONP-COOH and (B) IONP-drugs-FOL.

The stability of the fol-IONP-DOXO-OLA was studied over time in deionized water, PBS (phosphate buffer saline) and FBS (fetal bovine serum) (**Figure 6**). In order to study the stability, the size of the nanoparticles was measured after 1 day, 7 days, 30 days and 60 days. The size of the unconjugated nanoparticles fluctuated between 46nm to 46.89nm in deionized water, 47.18nm to 47.42mn in PBS, and 46.81nm to 47.37nm in FBS (**Figure 6A**). The size of the folate-conjugated nanoparticles encapsulated with drugs fluctuated between 51.15nm to 51.94nm in deionized water, 52.82nm to 51.63mn in PBS, and 51.81nm to 52.89nm in FBS (**Figure 6B**).

2.2.3 Cytotoxicity Studies:

The therapeutic efficacy and cytotoxicity of the drug-carrying nanoparticles was observed by MTT assay. Previous work shows that the fluorescence intensity of formazan crystals produced during MTT assay is directly proportional to the number of living cells in the sample. The viability of the LNCaP cells treated with doxorubicin, olaparib and the combination of the two was quantified via MTT assay. The viability was observed after treatment with the nanoparticle for both time dependence and dosage dependence. For the time dependent viability study for LNCaP cells (**Figure 7A**), the fluorescence after treatment was measured at 12 h, 24 h, 36 h, 48 h and was compared with the viability of the untreated cells. The viability of cells treated with individual drugs had noticeably reduced. Treatment with olaparib loaded IONP had more immediate effects with cell viability being reduced by 40% in 24h whereas cells treated with doxorubicin encapsulating IONP only had a reduction in viability of 23% within the same time. However, after 36h the doxorubicin-treated cells had an accelerated cell death with 40% viability at 36h compared to 45% with olaparib-treated cells. The cells treated with the combination of two drugs, however, had the most rapid reduction of cell viability, consistently throughout 48h duration of the study. The increase in cell death from combination treatment as opposed to the cell death from treatment with individual drugs is a demonstration of the synergistic effect. It is thought that PARP inhibitors like olaparib increase the ROS effects doxorubicin has on tumor cells. This synergetic effect in combination with the targeting modality of the folate conjugated IONPs makes for effective treatment while limiting the side effects on healthy cells that do not overexpress folate receptors. The viability assay done on PC3 cells treated with IONP-Doxo-Ola-Fol (**Figure 7B**) illustrated that the IONP-Doxo-Ola-Fols were not toxic to cells that do not have overexpressed folate receptors.

For the concentration dependent viability studies, the viability was quantified after 48 h from cell cultures treated with 25, 50, and 100 mM of therapeutic nanoparticle solution encapsulated with respective drugs (**Figure 8**) and compared with the control cells. The cells treated with both doxorubicin and olaparib together were shown to have more cell death than cells treated individually when the dosage was 25 mM and 50 mM. However, when the dosage was increased to 100 mM the cell death had little variance with different drug cocktails. However, in general it appeared that using the two drugs in combination increased the efficacy of the nanoparticles.

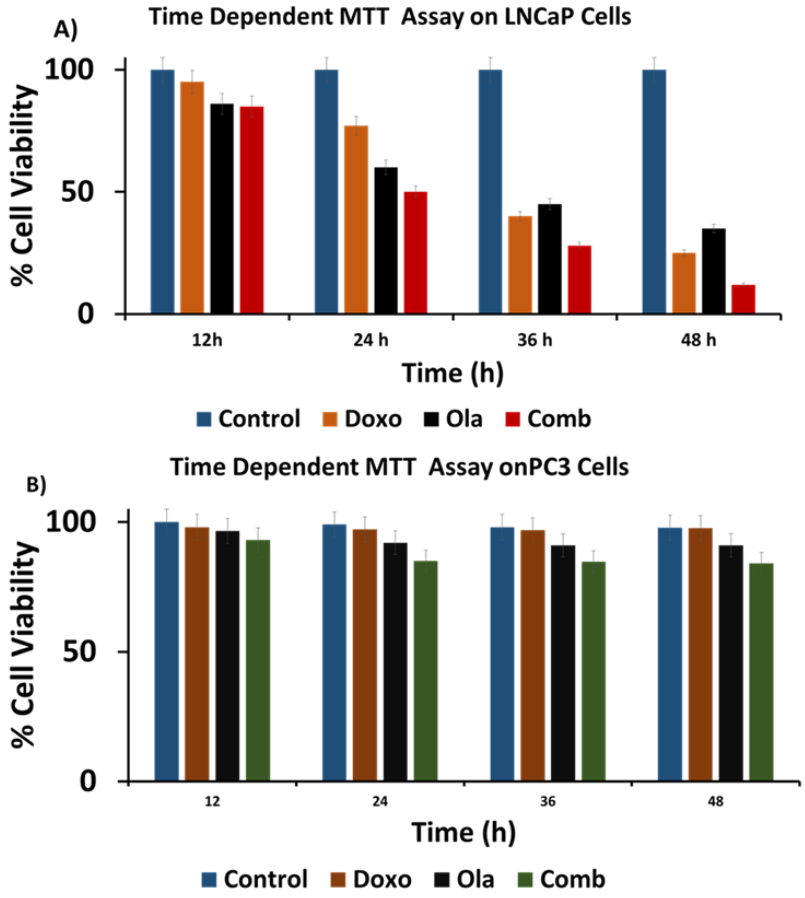

Figure 7: A) Time dependent MTT assay data for determination of cytotoxicity of IONP -FOL encapsulating drug cocktail as opposed to individual drugs for LNCaP cells, and B) PC3 cells for control.

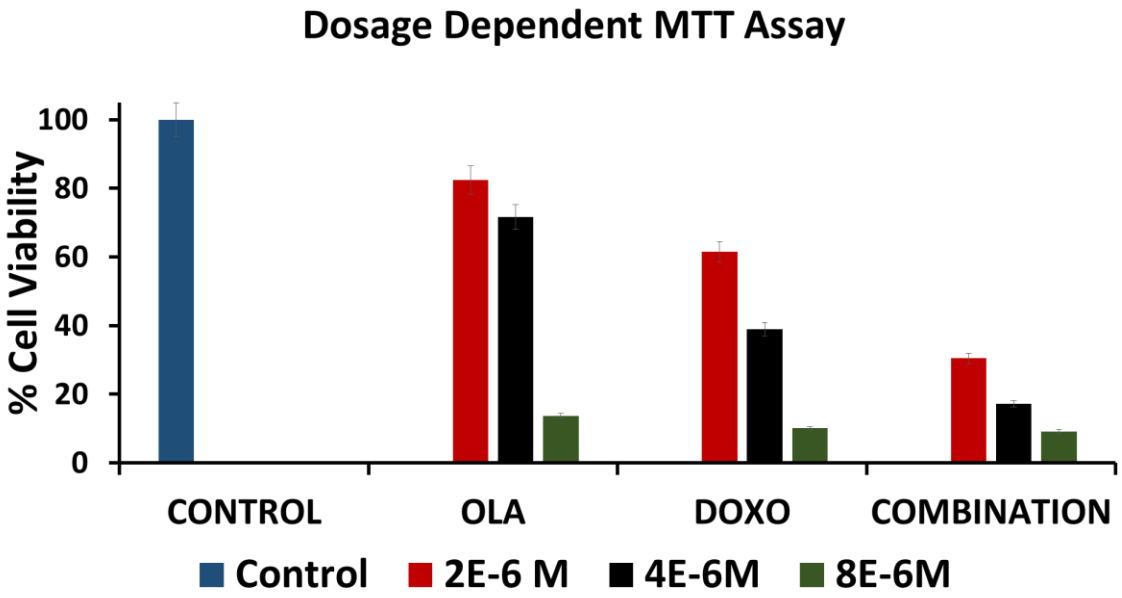

Figure 8: Concentration dependent MTT assay data for determination of cytotoxicity of IONP - FOL encapsulating drug cocktail as opposed to individual drugs. Fluorescent intensity measured at 595nm after 24 hours.

2.2.4 Cell Internalization Studies:

Following the cytotoxicity studies of the nanoparticles, further visualization of the cell death along with confirmation that the nanoparticles were entering the cell was desired. During the cell uptake studies, internalization of the drugs in the cells was observed alongside killing of the cells. Internalization of the doxorubin - IONP as well as combination of doxorubicin and olaparib - IONP were compared. **Figure 9A-D** show images taken 0 hours after treatment, **Figure 9E-H** show images taken 12hours after treatment, **Figure 9I-L** show images taken 24 hours after treatment, **Figure 9M-P** show images taken 36 hours after treatment, and **Figure 9Q-T** show images taken 48 hours after treatment. The internalization of the nanoparticles is observed under the red filter due to the fluorescent properties of doxorubicin and the nucleus is observed under the blue filter due to the DAPI dye staining. Red color in **Figure 9G, 9K** and **9O** shows the internalization of the nanoparticles at 12 h, 24 h and 48 h respectively whereas blue color in **Figure 9F, 9J** and **Figure 9N** shows staining of nucleus at 12 h, 24 h and 48 h respectively. The

decreased intensity of the blue light from 24h to 48 h is indicative of cell death. The results of the cell uptake study further demonstrate the cytotoxicity of the nanoparticles.

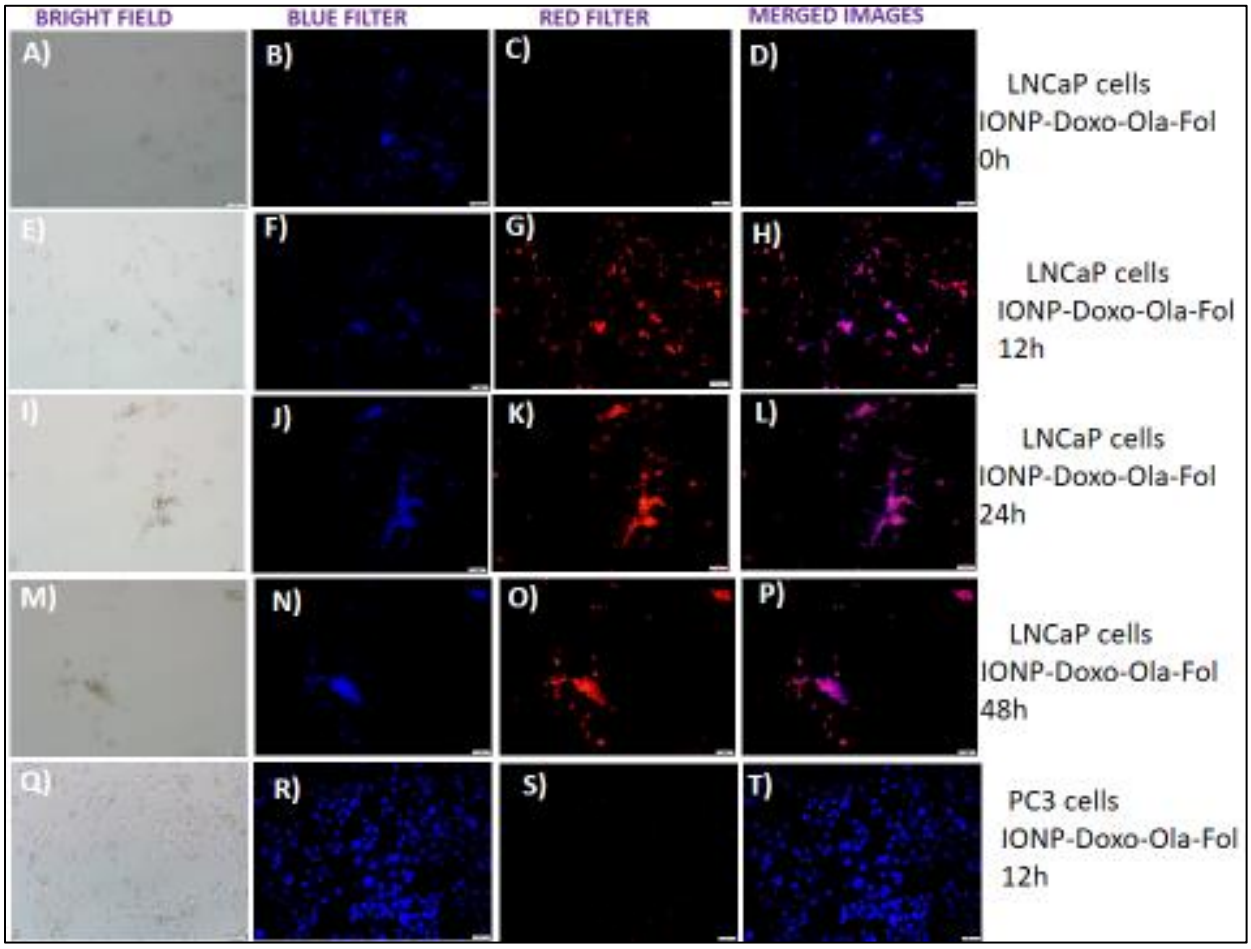

Figure 9: Cellular uptake studies of LNCaP cells: **Figures A-D** show the non-internalization, **Figures E-H** indicates the internalization, **Figures I-L** show the cell death at 24 h, **Figures M-P** shows the cell death at 48h, and **Figures Q-T** show the non-internalization of IONP-Doxo-Ola-Fol in PC3 Control Cells.

2.2.5 Studies of Reactive Oxidative Species Release:

Dihydroethidium (DHE) was used to observe the generation of reactive oxygen species (ROS). When the cell is undergoing oxidative stress, DHE is oxidized and converted to 2-hydroxyethidium in the nuclei which produces red fluorescence. This fluorescence was observed at 12, 24, 36, and 48 hours after treatment and the bright red color indicative of ROS was visible at each time point. A noticeable decrease in the number of cells every twelve hours indicated

that cells were dying. Previous work has shown that ROS generation is one of the main mechanisms of doxorubicin cytotoxicity towards tumor cells.[38-41] From the MTT assay **(Figure 7)**, it is shown when the LNCaP cells were treated with doxorubicin alone, acceleration of cell death was not observable until 36 hours after treatment, while cells treated with both doxorubicin and olaparib had expedited decrease in viability throughout the duration of the experiment. During the ROS studies, red fluorescence was weak at 12 hours (**Figure 10E**) but brighter at 24 hours (**Figure 10F**) indicating ROS generation increases over time. This shows that olaparib, a PARP inhibitor, causes doxorubicin to generate ROS at a much earlier time than if the cells were treated with doxorubicin alone. The synergetic effect of olaparib and doxorubicin is further demonstrated by the increased stress and decreased cell density observed at 36 hours (**Figure 10G**) and 48 hours (**Figure 10H**) after treatment. Treating the cells with encapsulated nanoparticles ensures that both drugs will intercalate within the DNA of the cancer cells.

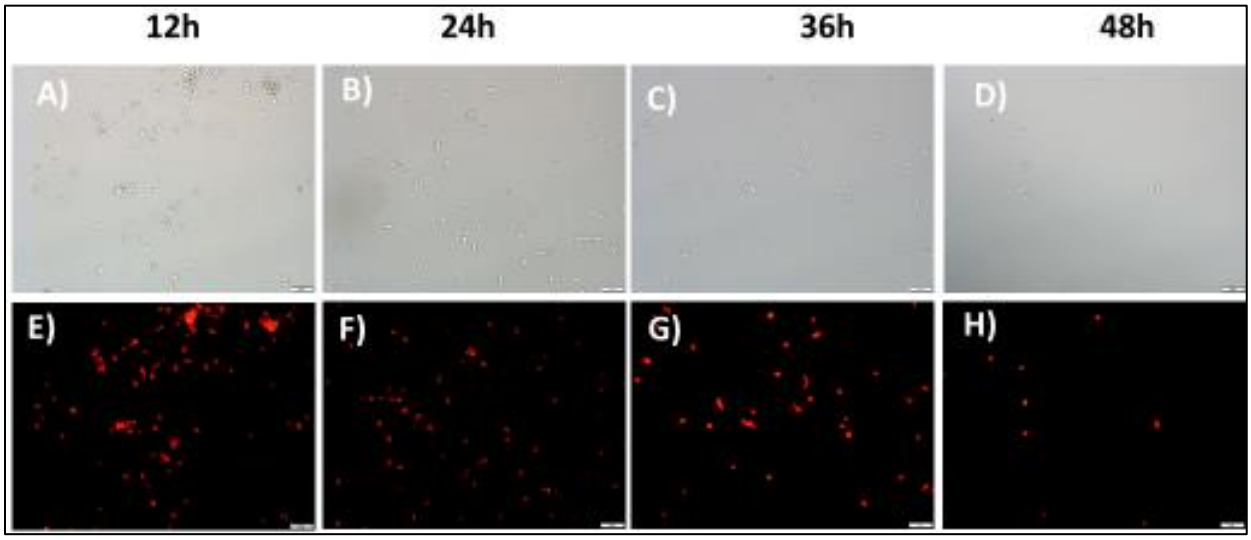

Figure 10: Measure of ROS generation in LNCaP cells at different time points including 12 h, 24 h, 36 h and 48 h, respectively in bright field(**A-D**) and corresponding red filter(**E-H**).

2.2.6 Programmed Cell death Studies:

The evidence of ROS generation prompted the observation of cell death mechanisms. To ensure the cell death was via apoptotic pathway, we performed apoptosis and necrosis assay which quantifies the cell death. Apoptosis, programmed cell death process, involves phosphatidyl serine moving from the inner leaflet of the plasma to the outer leaflet membrane.

Signs of apoptosis were observed after 12 h, 24 h, 36 h, and 48 h, as shown in the images taken in **Figure 11** and there was an observable reduction in the number of cells every twelve hours. The morphological change in the cells from needle to round shape were also observed which is indicative of apoptosis, and is noticeable from **Figures 11 A-D.**

Figure 11: Shows detection of apoptotic death at different time points in cells treated with

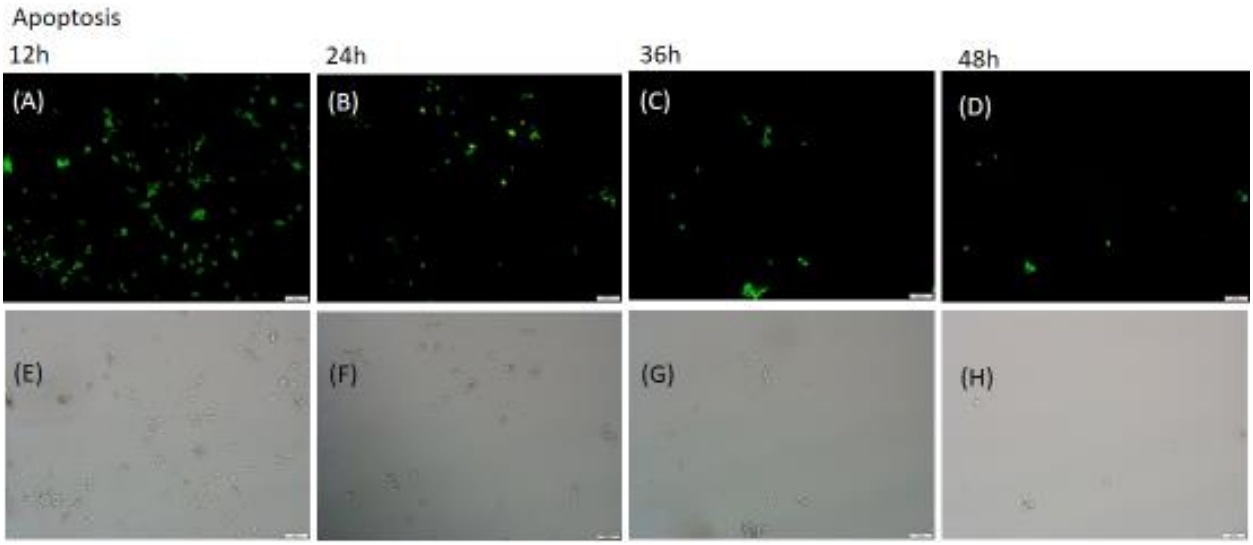

Doxorubicin and Olaparib encapsulated in folate conjugated IONPs. **Figures A-D** Show a decrease in number of cells and change in morphology over the course of 12, 24, 36, and 48 hours observed through the green filter of the microscope. **Figures E-H** shows the corresponding bright field.

2.2.7 DNA Damage Studies:

From literatures it is known that DNA damage is the mechanism of cytotoxicity for both olaparib and doxorubicin. The extent of the DNA damage was studied via comet assay with fluorescence microscope images shown in **Figure 12**. This was done for treatment with olaparib and doxorubicin separately as well as with treatment with a combination of the two. Treatment with olaparib resulted in the shortest tails(**Figure 12B**), followed by cells treated with doxorubicin having the second smallest tails(**Figure 12A**), and finally cells treated with the combination of the two having the longest tails (**Figure 12C**). The length of the tail is understood to be proportional to the extent of the DNA damage. The %DNA in the tail along with tail moment and olive tail moment were quantified via fluorescent intensity as shown in **Figure 13**. Cells treated with nanoparticles encapsulating both doxorubicin and olaparib were shown to have the most DNA in the tails on average, followed by cells treated with nanoparticles

containing only doxorubicin, and finally cells treated with nanoparticles loaded with only olaparib. Doxorubicin kills cells primarily via DNA damage, which explains why it would do more DNA damage than olaparib. The increase in DNA damage shown from the combination of the two is supportive of the proposed synergetic effect.

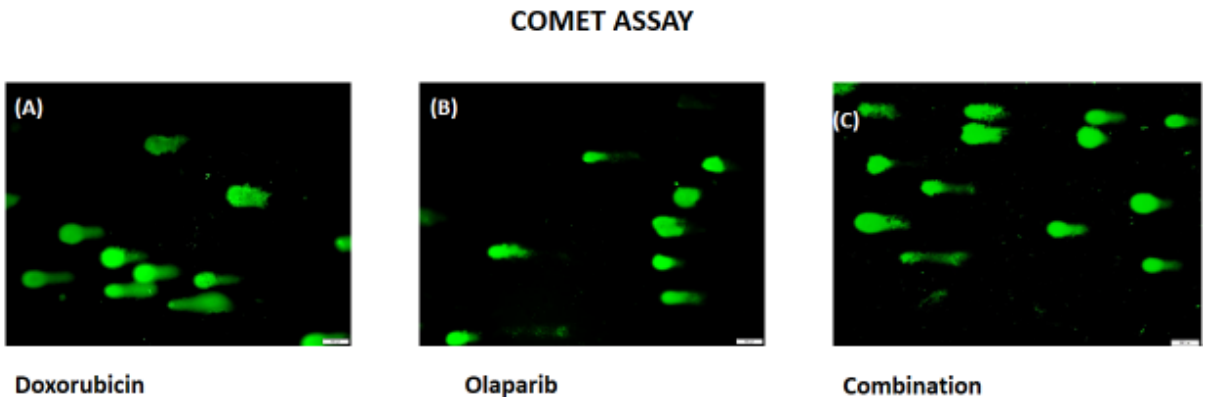

Figure 12: Shows DNA damage extent quantified via comet assay of cells treated with IONP-Fol nanoparticles that encapsulate A) doxorubicin B) olaparib and C) a drug cocktail consisting of both doxorubicin and olaparib.

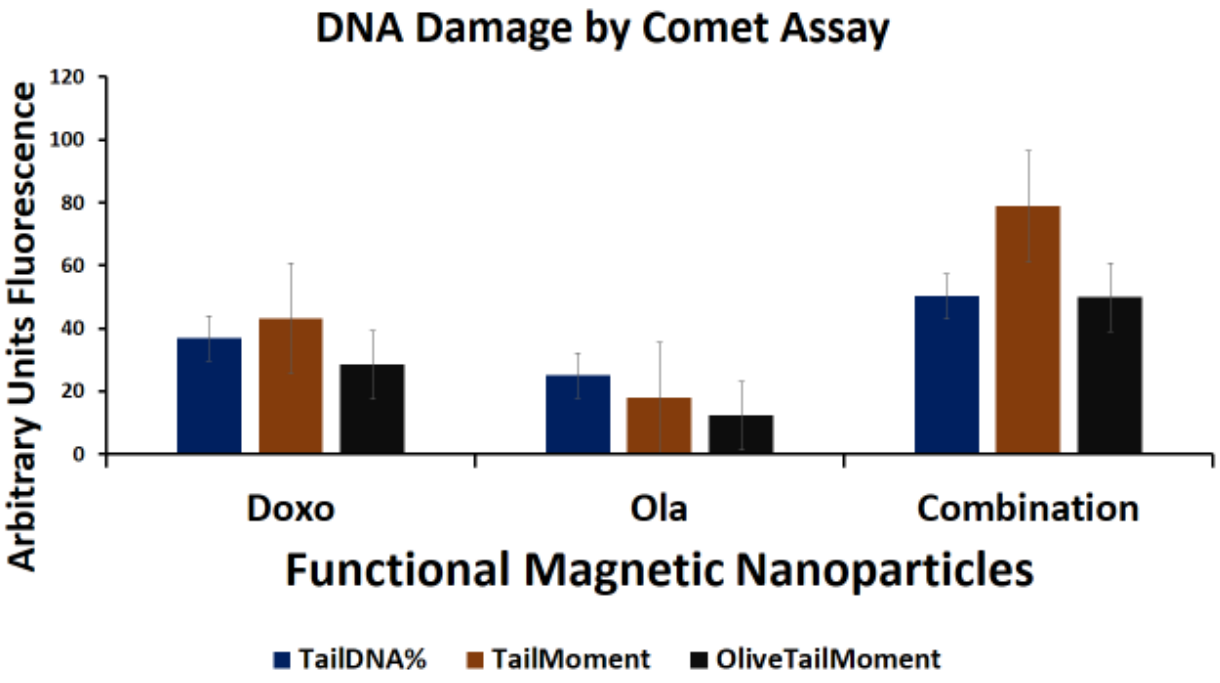

Figure 13: Shows quantified DNA damage extent quantified via comet assay of cells treated with

IONP-Fol nanoparticles that encapsulate doxorubicin, olaparib, and a drug cocktail consisting of both doxorubicin and olaparib.

2.2.8 Migration Assay:

The anti-metastatic potential of the therapeutic nanoparticles was observed via migration assay. The results for both untreated cells and cells treated with nanoparticles encapsulating the combination of doxorubicin and olaparib were compared. (**Figure 14**) The treated cells showed to have four times less migration than the untreated cells hence our nanoparticle encapsulated with drug cocktail has anti-metastatic property.

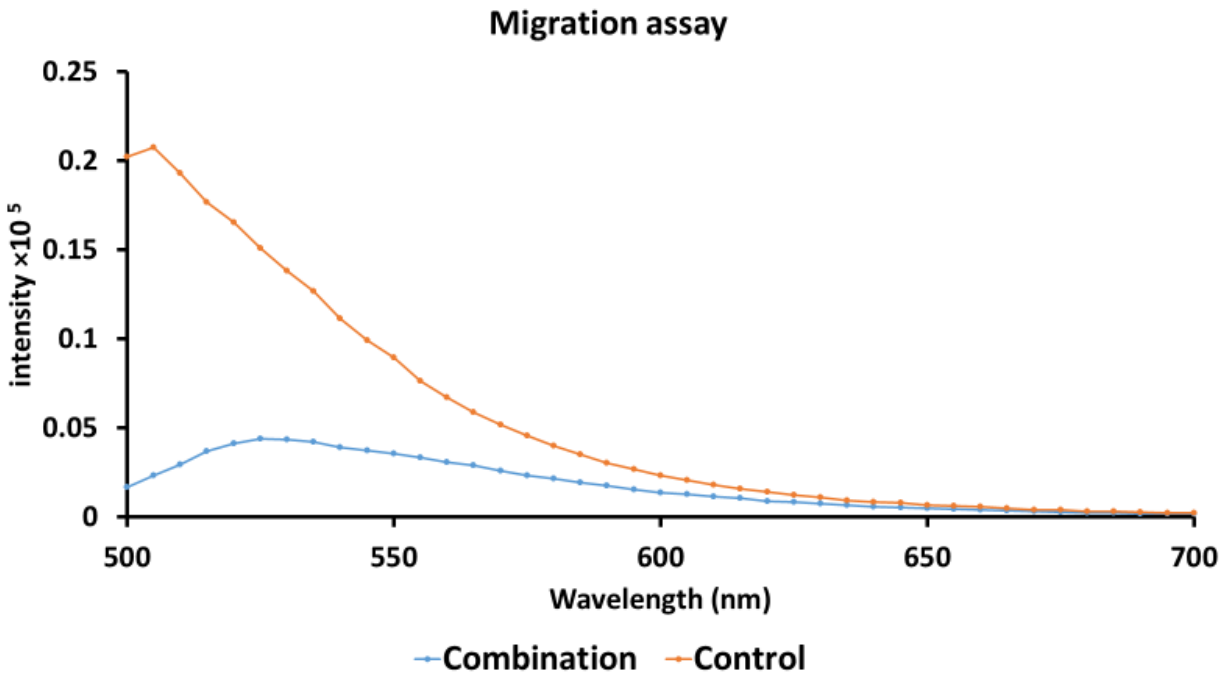

Figure 14: Displays the antimetastatic potential of IONP-Fol nanoparticles encapsulating doxorubicin and olaparib via migration assay.

2.2.9 Summary

The efficacy of olaparib and doxorubicin was shown to be improved by encapsulation in IONP-Fol. Results of cellular internalization, cytotoxicity and anti-metastatic potential studies were promising for analyzing the effectiveness of treatment against tumors. Evidence of increased ROS, apoptosis and DNA damage displayed the proposed synergetic effect of the combination of doxorubicin and olaparib for prostate cancer treatment. Future studies in vivo may show even further positive results to finally prompt clinical studies and finally shine hope on many prostate cancer patients in dire need for more effective treatment.

2.3 Experimental Methods:

2.3.1 Materials and Instruments

Ferric chloride, ferrous chloride, hydrochloric acid, ammonium hydroxide and PBS, were purchased from Fisher Scientific. Polyacrylic acid (PAA) was purchased form Sigma Aldrich. Doxorubicin was purchased from Alexis Biochemicals. 1-Ethyl-3-(3-dimethylaminopropyl)carbodiimide (EDC) was purchased from thermo Scientific. N-Hydroxysuccinimide (NHS) was purchased from Acros Organics. RPMI media, Antibiotic Antimycotic Solution (ABAM), and fetal bovine serum (FBS) were purchased from ATCC. 3-(4,5-dimethylthiazol-2-yl)-2,5-diphenyltetrazolium bromide MTT was purchased form MP Biomedical. Paraformaldehyde was purchased from Electron Microscopy Sciences. The Dihydroergotamine DHE dye was purchased from Cayman Chemicals as part of an ROS kit. The apoptosis kit was purchased from Biotium. The comet assay kit was purchased from Trevigen, as were LM agarose and lysis solutions. The SYBR gold dye was purchased from Invitroga by Thermo Fisher Scientific. The migration kit was purchased from Millipore.

The instruments used were a Malvern Zetasizer Nano ZS90 for average size and zeta potentials, a Tecan Infinite M200PRO plate reader for UV absorption and fluorescent intensity measurements, and an Olympus IX73 Fluorescence microscope for capturing images for cellular uptake, ROS, apoptotic studies and Comet assay.

2.3.2 Synthesis and Characterization

In order to synthesize the PAA coated IONPs, three solutions were prepared. Solution 1, consisted of $FeCl_3 \cdot 6H_2O$ (0.7540g), $FeCl_2 \cdot 4H_2O$ (0.374g), deionized water (2mL) and 12M HCl

(0.0089mL). Solution 2 consisted of 0.837g PAA and 5mL of deionized water. Solution 3 consisted of 30% NH_4OH(1.8mL) and 15mL of deionized water. Solution 1 was added to solution 3 while on a vortex of 850 rpm. Solution 2 was added to the mixture after 9 seconds with the vortex speed increasing to 3000 rpm. The product was then centrifuged at 3000rpm for 20 min, then twice more at 4000rmp for 20 min each. After each centrifugation, the top layer containing the smaller IONPs was collected while the bottom layer containing the unwanted larger IONPs was discarded. The product was then dialyzed for 24 hours in order to purify and remove the unreacted particles as well as nanoparticles that are of the undesired sizes.

The IONPs were folate conjugated via EDC/NHS chemistry followed by click chemistry. 31.2mg of EDC was mixed in 250mL MES buffer (pH 6.0) and was then added to 10mL of IONP solution. The mixture was mixed gently by rocking back and forth 20 times. 17.8mg of NHS was added to 250mL of MES buffer (pH 6.0) which was then mixed to the IONP solution in four parts of 60µL, and was gently mixed after each addition. 5mg of propargyl amine was added to 500µL of DMSO. This was added dropwise to the IONP/EDC/NHS mixture and was left on a table mixer for 3 hours. The mixture was then dialyzed in DI water for 2 hours to extract all unreacted materials.

Fol-NH_2 was dissolved in 0.5mL of water. The fol-NH_2 solution was added drop-wise to the IONP solution, and the solution was mixed four times after each drop. The solution was then dialyzed for 24 hours to remove any un-reacted reagents and other impurities.

Doxorubicin and olaparib were then co-encapsulated with the folate conjugated IONP using the solvent diffusion method. 5µL of doxorubicin (9mM) and 3µL of olaparib (11mM) were added to 250 mL of DMSO. The drug solution was then added dropwise to the 2mL of conjugated IONP solution while on the vortex. Each drop was 10 microliters in volume and the solution was vortexed for 45 seconds in between each drop. The mixture was then put on a mixer for 3 hours at 8 rpms. Un-encapsulated drug particles were removed via dialysis for 3 hours.

2.3.3 Cytotoxicity Studies:

The LNCaP cells used in this experiment were obtained from ATCC. The cells were cultured in composed of FBS, and ABAM mixed with nutrient media. Four cell cultures were incubated at 37°C in 96 well plates. One culture was untreated, one was treated with

doxorubicin alone, one with olaparib alone and one with the IONPs encapsulated with both drugs. The cells were then washed with 1X PBS, and then 30 µL MTT(5mg/L) was added. At the time points of 12, 24, 36, and 48 hours, the formation of formazan crystals was observed. These crystals were dissolved in isopropanol (10 mL isopropanol +250 µL). The absorbance was recorded with a Tecan i-control Plate reader at 570 nm.

2.3.4: Cell Internalization Studies

The optical modality of doxorubicin was utilized to observe the cellular internalization of the therapeutic IONPs using an Olympus Fluorescence microscope. As control LNCaP cells were treated with doxorubicin encapsulated with IONPs that were coated with PAA. Two other samples of LNCaP cells were treated with folate conjugated IONPS encapsulating doxorubicin alone for one sample, and the combination of doxorubicin and olaparib for the other sample. The fluorescence was observed for the control after 24 hours. The same was observed for cells treated with the IONPS encapsulating just doxorubicin after 24 hours and the cells treated with the drug combination after 24 hours and again after 48 hours.

2.3.5 ROS Studies:

The extent of cytosolic ROS was studied using DHE dye and a fluorescent microscope. The LNCaP cells were treated with the folate conjugated IONPS encapsulating the drug cocktail of doxorubicin and olaparib. The cells were incubated at 37 ^{o} C and the florescence was observed after 12, 24, 36, and 48 hours. The cells were washed with PBS and stained with DHE dye. Using the Olympus IX73 fluorescent microscope with the red filter the images for the cytosolic ROS generation were taken.

2.3.6 Programmed Cell Death Studies:

Apoptotic cells were observed using the Olympus fluorescence microscope and the Biotioum Apoptosis & Necrosis Quantification Kit. The cells were treated with the folate conjugated IONPs encapsulating the drug combination of doxorubicin and olaparib. The cells were incubated at 37 ^{o} C. The cells were washed twice with PBS, then stained with Annexin V-FITC (5µL) and Ethidium Homodimer (III)(5 µL). They were then washed with annexin B binding buffer twice and fixed with 4% paraformaldehyde. The fluorescent images were taken after 12, 24, 36 and 48 hours after using the Olympus IX73 fluorescence microscope. The green images indicate apoptotic cells, and red images indicate necrotic cells.

2.3.7 DNA Damage studies

The comet assay was conducted using a Trevigen comet assay kit. 100 µL of a mixture of LNCaP cells and LM agarose was placed in the wells of the pretreated comet slides. The slides were left in the dark for 30 min. Thereafter, the cells were immersed in lysis solution at 4 ◦C overnight. The excess buffer was then drained out of the slide. The slides were then immersed in an alkaline unwinding solution. A black cathode of 21 Volts was used for alkaline electrophoresis for 30 min. Any excess electrophoresis solution was removed. The slide was rinsed in deionized water twice for five minutes, and then 70% ethanol solutions for five minutes. The slides were mixed on a thermo mixer for ten to fifteen minutes at 37^{o} C. 100 µL of SYBR gold was used to stain the cells in each well. Deionized water was used to rinse out any excess dye. After drying, the IX73 Olympus fluorescence microscope was used to capture fluorescent images.

2.3.8 Antimetastatic Potential:

A Chemicon QCM 96-well cell migration assay kit from Millipore was used. The serum-starved cells were incubated for 24 hours in a 70mL flask. Some cells were then treated were folate conjugated IONPs encapsulating doxorubicin and olaparib while, the other cells were treated with PBS for control. The cells were seeded in the invasion chamber and coated with DMEM. The feeding tray was loaded with 10% FBS. The cells were then allowed to migrate and incubated for 24 hours. The slide was then treated with lysis buffer and CYQuant dye. The cells were then transferred to another well. Fluorescence intensity was measured at 480/520 nm wavelength using a Tecan i-control plate reader.

Chapter III

Conclusion and Future Direction

The highly metastatic nature of prostate cancer had caused the treatment of such cancer to be an overwhelming challenge as of current day. Chemotherapy alone is not sufficient in treating the cancer, thus more invasive procedures such as surgical castration and radiation therapy are usually employed, thus providing the patient with an excessively stressful experience for an already terrifying illness.

Nanotechnology based drug delivery offers a much more effective treatment regimen. The targeting of drugs allows for less inappropriate accumulation of the drug in healthy cells, which would reduce the extent of the negative side effects on the patient's health. The amount of drug molecules that actually enter the targeted cells is much higher when nanoparticles are used for delivery than they are if the drugs are administered via the conventional method. Drugs are protected from undergoing degradation outside of the target site if they are encapsulated in nanoparticles. The size of the nanoparticles (1-100nm) allows for them to easily enter and exit from healthy cells, thus making them amply biocompatible.

In this study multimodal nanoparticles for targeting prostate cancer were synthesized. Iron oxide nanoparticles coated with PAA were synthesized. The particles were then functionalized with folate using EDC/NHS and click chemistry in order to target folate receptors that are over expressed in prostate cancer cells. The cancer drugs, doxorubicin and olaparib, were then encapsulated into the nanoparticles using the solvent diffusion method. The particles were purified via dialysis, and then characterized for their size, zeta potential, UV fluorescence and absorption via DLS and UV fluorescence. The size was also found to be stable over the course of 60 days which is as long as a typical chemotherapy cycle.

The internalization of the nanoparticles in LNCaP cells was studied via fluorescence microscopy. The particles were shown to have entered the cell after 12 hours. Cell death was observable after 24 hours and more so after 48 hours. The cytotoxicity of the nanoparticles was observed by quantifying the viability of treated cells via MTT assay. The viability of cells treated with olaparib alone decreased at a higher rate than that of cells treated with doxorubicin alone between 0 and 24 hours after treatment. However, the viability of cells mono-treated with doxorubicin had dropped below that of cells mono-treated with olaparib 36 hours after treatment. The cells treated with the combination of the two drugs had significantly lower viability than all other cells, supporting the proposed synergistic effect of treatment with doxorubicin and olaparib together. The release of reactive oxygen species was also observed via fluorescence microscopy. Over the course of 48 hours after treatment with the nanoparticles, the presence of reactive oxygen species was detected along with noticeable cell death. The mechanism of cell death was found to be primarily apoptotic. The extent of DNA damage from cells treated with doxorubicin, olaparib and the combination of the two were observed via comet assay. The combination of the two drugs was shown to cause more DNA damage than treatment with either drug individually, which supports the proposed synergistic effect. Finally, the anti-metastatic potential of the nanoparticles was studied via migration assay. The drugs were found to be promisingly anti-metastatic. The IONP-Fol nanoparticles encapsulating doxorubicin and olaparib provide promise for more effective treatment of cancer in the future. Further studies *in-vivo* and in clinical settings would provide more confidence in the use of these particles. Another study involving IONP-Fol particles encapsulating folate functionalized prodrugs of doxorubicin and olaparib could potentially show further protection from drug degradation outside of the target site as well as even further reduction of side effects.

REFERENCES

1) https://www.cancerresearchuk.org/about-cancer/prostate-cancer/types-grades
2) https://www.medicalnewstoday.com/articles/297516.php
3) https://www.webmd.com/prostate-cancer/news/20150731/five-types-prostate-cancer
4) https://www.cancer.org/cancer/prostate-cancer/about/what-is-prostate-cancer.html
5) https://prostatecancer.net/basics/types/
6) https://www.cancercenter.com/prostate-cancer/types/
7) Tavora, F., Epstein, J., High-grade Prostatic Intraepithelial Neoplasialike Ductal Adenocarcinoma of the Prostate: A Clinicopathologic Study of 28 Cases *The American Journal of Surgical Pathology* **2008** *32* 1060-1067
8) P A Humphrey https://jcp.bmj.com/content/60/1/35.short
9) https://www.cancer.org/cancer/prostate-cancer.html
10) https://www.cancer.org/cancer/prostate-cancer/treating.html
11) https://www.pcf.org/about-prostate-cancer/prostate-cancer-treatment/
12) https://www.webmd.com/prostate-cancer/guide/prostate-cancer-treatment-care
13) https://www.cancer.net/cancer-types/prostate-cancer/types-treatment
14) https://www.mayoclinic.org/diseases-conditions/prostate-cancer/diagnosis-treatment/drc-20353093
15) https://www.cancercenter.com/prostate-cancer/diagnostics-and-treatments/tab/treatment-options/
16) https://www.cancer.gov/types/prostate/patient/prostate-treatment-pdq
17) https://www.urologyhealth.org/urologic-conditions/prostate-cancer/treatment
18) https://www.cancer.org/cancer/prostate-cancer/treating/chemotherapy.html
19) Petrylak, D,. Tangen, C., Hussain, M. Docetaxel and Estramustine Compared with Mitoxantrone and Prednisone for Advanced Refractory Prostate Cancer *The New England Journal of Medicine* **2004**
20) Paller, C., Antonarakis, E. Cabazitaxel: a novel second-line treatment for metastatic castration-resistant prostate cancer. *NCBI* **2011** *5* 117-124
21) Lammers, T., Kiessling, F., Hennink, W., Storm, G. Nanotheranostics and Image-Guided Drug Delivery: Current Concepts and Future Directions. *ACS Publications* **2010** *7* 1899-1912
22) Kunjachan, S., Ehling, J., Storm, G., Kiessling, F., Lammers, T.(Noninvasive Imaging of Nanomedicines and Nanotheranostics: Principles, Progress, and Prospects *ACS Publications* **2015** *115* (19), 10907-10937
23) ElBayoumi, T., Rorchilin, P. (2009) Tumor-Targeted Nanomedicines: Enhanced Antitumor Efficacy In vivo of Doxorubicin-Loaded, Long-Circulating Liposomes Modified with Cancer-Specific Monoclonal Antibody. *AACR Publications*. **2015** *15* 1845-2203.

24) Shapira, A., Livney, Y., Broxterman, H. Nanomedicine for targeted cancer therapy: Towards the overcoming of drug resistance *Dimensions* **2011** *14* 150-163
25) Wicki, A., Witzigmann, D., Balasubramanian, V., Huwyler, J. *Elsevier* **2015** *200* 138-157
26) XU,X., Ho, W., Betrand, N., Farokhzad, O. (2015) Cancer nanomedicine: from targeted delivery to combination therapy. *Europe PMC* **2015** *21* 223-232
27) Nagesh, P.K.B., Johnson, N.R., Boya, V.K.N., Chowdhury, P., Othman, S.F. PSMA targeted docetaxel-loaded superparamagnetic iron oxidenanoparticles for prostate cancer. *Nanomedicine.* **2016** *144* 8-20
28) Meidanchi, A., Akhavan, O., Khoei, S., Shokri, A. A., Hajikarimi, Z., & Khansari, N. (2015). ZnFe2O4 nanoparticles as radiosensitizers in radiotherapy of human prostate cancer cells. *Materials Science and Engineering: C*, *46*, 394-399.
29) Yallapu, M. M., Khan, S., Maher, D. M., Ebeling, M. C., Sundram, V., Chauhan, N., ... & Jaggi, M. (2014). Anti-cancer activity of curcumin loaded nanoparticles in prostate cancer. *Biomaterials*, *35*(30), 8635-8648.
30) Yan, J., Wang, Y., Zhang, X., Liu, S., & Tiana, C. Targeted nanomedicine for prostate cancer therapy: Docetaxel and curcumin co-encapsulated lipid–polymer hybrid nanoparticles for the enhanced anti-tumor activity in vitro and in vivo. *Drug Delivery*. **2015** *23(5)* 1757-1762
31) Meidanchi, A., Akhavan, O., Khoei, S., Shokri, A. A., Hajikarimi, Z., & Khansari, N. (2015). ZnFe2O4 nanoparticles as radiosensitizers in radiotherapy of human prostate cancer cells. *Materials Science and Engineering C,46*, 394-399.
32) Tse, B., Cowin, J.C., Soekmadji, C., Jovanovic, L., Vasireddy, R., Ling, M. Khatri, A. Liu, T., Thierry, B., Russel, P. (2015). PSMA-targeting iron oxide magnetic nanoparticles enhance MRI of preclinical prostate cancer. *Nanomedicine.* **2015** *10(3)* 375-386
33) Nagesh, P. K., Johnson, N. R., Boya, V. K., Chowdhury, P., Othman, S. F., Khalilzad-Sharghi, V., ... & Zafar, N. (2016). PSMA targeted docetaxel-loaded superparamagnetic iron oxide nanoparticles for prostate cancer. *Colloids and Surfaces B: Biointerfaces*, *144*, 8-20
34) Kaufman, B., Shapira-Frommer, R., Schmutzler, R. K., Audeh, M. W., Friedlander, M., Balmaña, J., ... & Rosengarten, O. (2015). Olaparib monotherapy in patients with advanced cancer and a germline BRCA1/2 mutation. *Journal of clinical oncology: official journal of the American Society of Clinical Oncology*, *33*(3), 244.
35) Tacar, O., Sriamornsak, P., & Dass, C. R. (2013). Doxorubicin: an update on anticancer molecular action, toxicity and novel drug delivery systems. *Journal of Pharmacy and Pharmacology*, *65*(2), 157-170.
36) Kumar, S., Marfatia, R., Tannenbaum, S., Yang, C., Avelar, E. (2012) Doxorubicin-Induced Cardiomyopathy 17 Years after Chemotherapy. *Texas Heart Institute Journal.*
37) https://www.sigmaaldrich.com/catalog/product/sigma/d1515?lang=en&region=US
38) https://www.urologyhealth.org/urologic-conditions/prostate-cancer/treatment
39) Fong, M. Y., Jin, S., Rane, M., Singh, R. K., Gupta, R., & Kakar, S. S. (2012). Withaferin A synergizes the therapeutic effect of doxorubicin through ROS-mediated autophagy in ovarian cancer. *PloS one*, *7*(7), e42265.
40) Wang, J., & Yuan, Z. (2013). Gambogic acid sensitizes ovarian cancer cells to doxorubicin through ROS-mediated apoptosis. *Cell biochemistry and biophysics*, *67*(1), 199-206.

41) Chao, H., Liu, J., Hong, H., Lin, J., Chen, C., Cheng, T., (2011) L-carnitine reduces doxorubicin-induced apoptosis through a prostacyclin-mediated pathway in neonatal rat cardiomyocytes. *International journal of cardiology*, *146*(2), 145-152.
42) Santra, S.; Kaittanis, C.; Grimm,J.; Perez,J.; Drug/Dye-Loaded, Multifunctional Iron Oxide Nanoparticles for Combined Targeted Cancer Therapy and Dual Optical/Magnetic Resonance Imaging *Small, 5(16), 1862-1868.*
43) Langelier, M. F., & Pascal, J. M. (2013). PARP-1 mechanism for coupling DNA damage detection to poly (ADP-ribose) synthesis. *Current opinion in structural biology*, *23*(1), 134-143.